

# Interactions in the Sol–Gel Processing of Alumina–Zirconia Composites

V. Srdić & L. Radonjić

Department of Inorganic Technology and Materials, Faculty of Technology, Bul. Cara Lazara 1, 21000 Novi Sad, Yugoslavia

(Received 7 July 1993; revised version received 7 March 1994; accepted 15 March 1994)

## Abstract

*The combined effect of alumina and zirconia on the phase transformation and microstructure development of heat-treated alumina–zirconia composites has been studied. The composites were prepared by the sol–gel process, using two different alumina matrices (polymer and particulate) and three different types of zirconia particles. The influence of the different zirconia particles on the phase transformation and microstructure development of the alumina matrix is clearly evident. In addition, stability of tetragonal zirconia in the alumina matrix is considerably changed, in respect to pure zirconia powder. These effects are explained by the existence of a mutual interaction between the zirconia and the transitional aluminas, which is stronger if the alumina and zirconia particles are smaller and more intimately mixed.*

*Der Kombinationseffekt von Aluminium- und Zirkoniumoxid auf die Phasentransformation und die Entwicklung des Gefüges von wärmebehandelten Aluminiumoxid–Zirkoniumoxid-Verbundwerkstoffen wurde untersucht. Die Herstellung der Verbundwerkstoffe erfolgte mittels der Sol–Gel-Methode unter Verwendung zweier verschiedener Aluminiumoxidmatrizen (polymer- und teilchenförmig) und dreier verschiedener Typen Zirkoniumoxidteilchen. Der Einfluß der verschiedenen Zirkoniumoxidteilchen auf die Phasentransformation und das Gefüge der Aluminiumoxidmatrix ist klar ersichtlich. Die Stabilität des tetragonalen Zirkoniumoxids in der Aluminiumoxidmatrix hat sich, im Vergleich zu reinem Zirkoniumoxidpulver, erheblich verändert. Diese Effekte lassen sich auf die vielfältigen Wechselwirkungen zwischen Zirkoniumoxid und den Übergangsaluminiumoxyden zurückführen. Die Wechselwirkung ist stärker, wenn die Aluminium- und Zirkoniumoxidteilchen kleiner und besser vermischt sind.*

*Les auteurs ont étudié l'effet combiné de l'alumine et de la zircone sur la transformation de phase et le développement de la microstructure de composites alumine–zircone. Les composites ont été préparés par la méthode sol–gel, en utilisant deux matrices d'alumine différentes (polymère et particulaire) et trois types de particules de zircone différentes. L'influence des particules de zircone différentes sur la transformation de phase et sur le développement de la microstructure est tout-à-fait évidente. En outre, la stabilité de la zircone quadratique dans la matrice en alumine est considérablement modifiée par rapport à la poudre de zircone pure. Ces effets sont expliqués par l'existence d'une interaction mutuelle entre la zircone et les aluminas de transition, qui est plus forte si des particules d'alumine et de zircone sont plus petites et mélangées plus intimement.*

## Introduction

The fracture toughness and strength of alumina ceramics can be significantly increased by utilizing the martensitic tetragonal (t) to monoclinic (m) phase transformation of zirconia particles dispersed in the alumina matrix.<sup>1–4</sup> The magnitude of toughening is complexly dependent on the alumina–zirconia composite microstructure (volume fraction of zirconia particles, the size, shape, location and size distribution and amount of metastable tetragonal zirconia).<sup>4–6</sup>

The sol–gel process has potential for the fabrication of these composites,<sup>7–13</sup> because of the homogeneous mixing of the two phases at a very fine scale, the fine-grained microstructure and the relatively low sintering temperatures. However, there are many unresolved problems in the processing of sol–gel alumina–zirconia composites. For example, the control of microstructure development in the alumina matrix is complicated by the existence of many metastable alumina phases.

Other problems relate to the zirconia particles, i.e. their particle size, distribution and crystalline structure.<sup>4-6</sup> In addition, there are experimental results,<sup>8,9</sup> which show that mixing at a very fine scale, characteristic for the sol-gel process, also causes a coupled interaction between the alumina and zirconia, i.e. the phase transformations and grain growth of both are mutually related and determine the final composite microstructure.

The aim of this study is to elucidate the mutual interaction between the alumina matrix and the zirconia particles in sol-gel derived alumina-zirconia composites. To achieve this goal, two different alumina matrices were used (polymer and particulate) and three different types of zirconia particles.

## 2 Experimental

Four different alumina-zirconia composites with 20 wt% ZrO<sub>2</sub> on an oxide basis were made (Table 1). Aluminium sec-butoxide, Al<sup>S</sup>Bu, and boehmite powder (Advanced Ceramic H-3500, Union Carbide, Cleveland, OH) were used for the preparation of two different types of composites: polymer matrix and particulate matrix composites, respectively. Also, zirconium *n*-propoxide, Zr<sup>n</sup>Pr, and zirconium oxychloride, ZrOCl<sub>2</sub>, were used for the introduction of the zirconia.

Polymer matrix sol (denoted by B<sub>o</sub>) was prepared by hydrolysis of Al<sup>S</sup>Bu after the method of Yoldas.<sup>14,15</sup> Peptization of aluminium hydroxide, in the 2·1-B<sub>o</sub> sol (Table 1), was carried out with ZrOCl<sub>2</sub>/water solution at *T* = 80°C, under reflux and with vigorous stirring. In the second 3·1-B<sub>o</sub> polymer matrix composite (Table 1), the alumina sol is the same as in the 2·1-B<sub>o</sub> sample except in that nitric acid was used for peptization. Zirconia sol, introduced into this polymer alumina sol B<sub>o</sub>, was prepared by hydrolysis of Zr<sup>n</sup>Pr, dissolved in anhydrous ethanol (0·4 mol Zr<sup>n</sup>Pr/litre)

under acid conditions, at ambient temperature (alkoxide : water : acid molar ratio was 1 : 6 : 1).

The set of particulate matrix composite sols were prepared from particulate alumina sol (denoted by A<sub>o</sub>). This sol was made by dispersing 20 wt% boehmite powder in distilled water with nitric acid at pH = 3 and at room temperature. In the particulate alumina sols, two types of zirconia sols were mixed. These zirconia sols are expected to have a difference in zirconia particle size on the basis of previous experiments.<sup>16</sup> In the first composites, denoted by 3·1-A<sub>o</sub> (Table 1), the same zirconia sol as in the polymer matrix composite 3·1-B<sub>o</sub> was used, whereas in the second, denoted by 3·2-A<sub>o</sub> (Table 1), the zirconia sol was prepared with the same conditions as for 3·1-B<sub>o</sub> and 3·1-A<sub>o</sub> samples, except that the alkoxide : water : acid molar ratio was 1 : 1 : 0.

In addition, α-alumina seeded composites were also prepared according to a published procedure.<sup>17</sup> In the sample notation the seeded samples have index 'c' in place of 'o'.

The prepared sols were gelled by heating at 70°C. The gels were aged at room temperature and carefully dried (because of the small cracking resistance of the polymer matrix gels 2·1-B<sub>o</sub> and 3·1-B<sub>o</sub>) in air for a few days at temperatures up to 120°C. Air dried gel fragments were first heated at 600°C for 1 h, then at 1150°C (or 1200°C) for 1 h and finally at up to 1400°C for 1 h.

The X-ray diffraction data were obtained on a diffractometer using Ni-filtered CuK<sub>α</sub> radiation. The ratio of t/m ZrO<sub>2</sub> was determined using the integrated intensity of the tetragonal (111) and monoclinic (111) and (11 $\bar{1}$ ) peaks.<sup>18</sup> The X-ray crystal size of the heat-treated samples was determined by the Scherrer formula.<sup>19</sup> The microstructural features of freshly fractured surfaces, slightly etched, were observed using a scanning electron microscope JEOL 035.

Table 1. Sample notation

Precursor for ZrO <sub>2</sub>	Polymer matrix composite	Particulate matrix composite
	Precursor for Al <sub>2</sub> O <sub>3</sub>	
	Al <sup>S</sup> Bu	Boehmite powder
Zr <sup>n</sup> Pr	3·1-B <sub>o</sub> <sup>a</sup>	3·1-A <sub>o</sub> <sup>a</sup>
ZrOCl <sub>2</sub>	—	3·2-A <sub>o</sub> <sup>b</sup>
	2·1-B <sub>o</sub>	—

<sup>a</sup>Zirconia sol prepared under acid condition with alkoxide : water : acid molar ratio 1 : 6 : 1.

<sup>b</sup>Zirconia sol prepared with alkoxide : water : acid molar ratio 1 : 1 : 0.

## 3 Results and Discussion

### 3.1 Gelation behaviour and microstructure of the composite gels

The gelation behaviour of the polymer matrix and the particulate matrix composites is quite different. The solid concentration at the gel point (Table 2), of the 2·1-B<sub>o</sub> and 3·1-B<sub>o</sub> samples is much higher than for the other two gels, indicating that the polymer matrix gels contain a very high amount of liquid and thus are very sensitive to drying. This results in a lower cracking resistance in the polymer matrix gels.

The dried particulate matrix gels are opaque in contrast to the polymer matrix gels which are

**Table 2.** Characteristics of composite gels

Sample notation	Solid concentration at gel point (wt%)	Mass of dried gel in relation to the theoretical mass <sup>a</sup>	Density of dried gel (g/cm <sup>3</sup> )
2·1-B <sub>0</sub>	4·0	1·31	2·34
3·1-B <sub>0</sub>	4·9	1·33	2·29
3·1-A <sub>0</sub>	11·2	1·08	1·94
3·2-A <sub>0</sub>	14·7	1·04	1·62

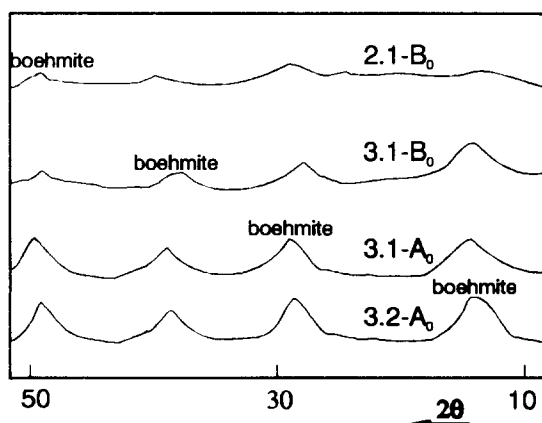
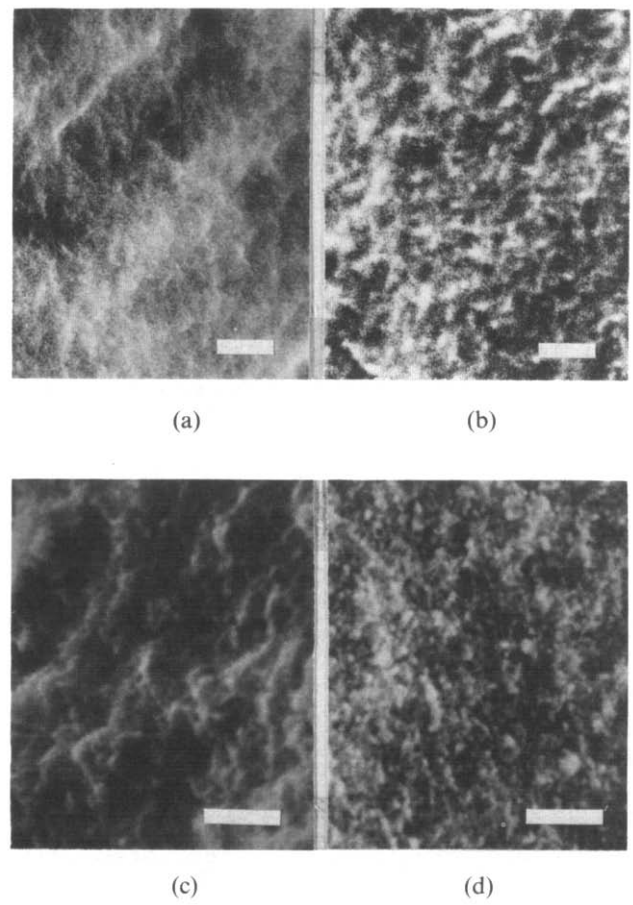
<sup>a</sup> Theoretical mass was calculated on the basis of  $\gamma$ -AlOOH and ZrO<sub>2</sub>.

translucent. All the dried composite gels have a crystalline boehmite-like structure more or less well developed (the 2·1-B<sub>0</sub> being the least crystalline), but without any traces of zirconia phases (Fig. 1). The density and mass of the dried gels are presented in Table 2, and the microstructure is shown in Fig. 2. The 3·2-A<sub>0</sub> gel has the lowest density and the mass of the dried gel is near to the theoretical mass, as is that of the 3·1-A<sub>0</sub> sample (Table 2). The microstructures of the particulate matrix composites, 3·1-A<sub>0</sub> and 3·2-A<sub>0</sub>, are similar (Fig. 2(c) and (d)). They have rather coarse particulate microstructures (in respect to the polymer one), but it is still not possible to distinguish zirconia particles in it. The polymer matrix dried gels 2·1-B<sub>0</sub> and 3·1-B<sub>0</sub> have higher density, and higher mass in respect to the theoretical mass (Table 2). The microstructure of these composites (Fig. 2(a) and (b)) is more diffuse than for the particulate matrix composites.

### 3.2 Phase transformations of alumina and zirconia in the heated composite samples

The phase transformations of all alumina-zirconia composites after heating are presented in Figs 3 and 4.

In the 2·1-B<sub>0</sub> composite at 600°C, only the  $\gamma$ -phase of alumina is found (Fig. 3); this persists to temperatures even above 1000°C. With increasing temperature, the  $\gamma$ -alumina gradually disappears,

**Fig. 1.** X-Ray diffraction of alumina-zirconia composite gels.**Fig. 2.** SEM micrographs of the alumina-zirconia composite gels: (a) 2·1-B<sub>0</sub>, (b) 3·1-B<sub>0</sub>, (c) 3·1-A<sub>0</sub> and (d) 3·2-A<sub>0</sub> (bar = 0·5  $\mu$ m).

while the diffraction peaks characteristic for the  $\theta$ -alumina become apparent. Transformation of the  $\theta$ - to  $\alpha$ -alumina begins at above 1200°C; even at 1250°C the  $\theta$ -alumina has not completely transformed. In contrast to pure alkoxide-derived alumina,<sup>20</sup>  $\gamma$ -alumina is less well defined and transforms to  $\theta$ -alumina and then to  $\alpha$ -alumina at 100°C and 150°C higher temperatures than in the pure system, respectively (Table 3). On the other hand, zirconia in the 2·1-B<sub>0</sub> composite crystallized first in the tetragonal form at 900°C (Fig. 3), a much higher temperature than usual for pure zirconia powder.<sup>21-23</sup> Since the zirconia particles are very small (Table 4), zirconia completely

**Table 3.** The started temperatures at the  $\theta$ - to  $\alpha$ -alumina phase transformation

Sample notation	$\theta$ - to $\alpha$ -Alumina starting temperature (°C)
Pure alkoxide derived alumina (B <sub>0</sub> ) <sup>a</sup>	1050
Pure particulate alumina (A <sub>0</sub> ) <sup>b</sup>	1100
3·2-A <sub>0</sub>	1150
3·1-A <sub>0</sub>	1150
3·1-B <sub>0</sub>	1170
2·1-B <sub>0</sub>	1200

<sup>a</sup> According to Ref. 20.

<sup>b</sup> According to Ref. 24.

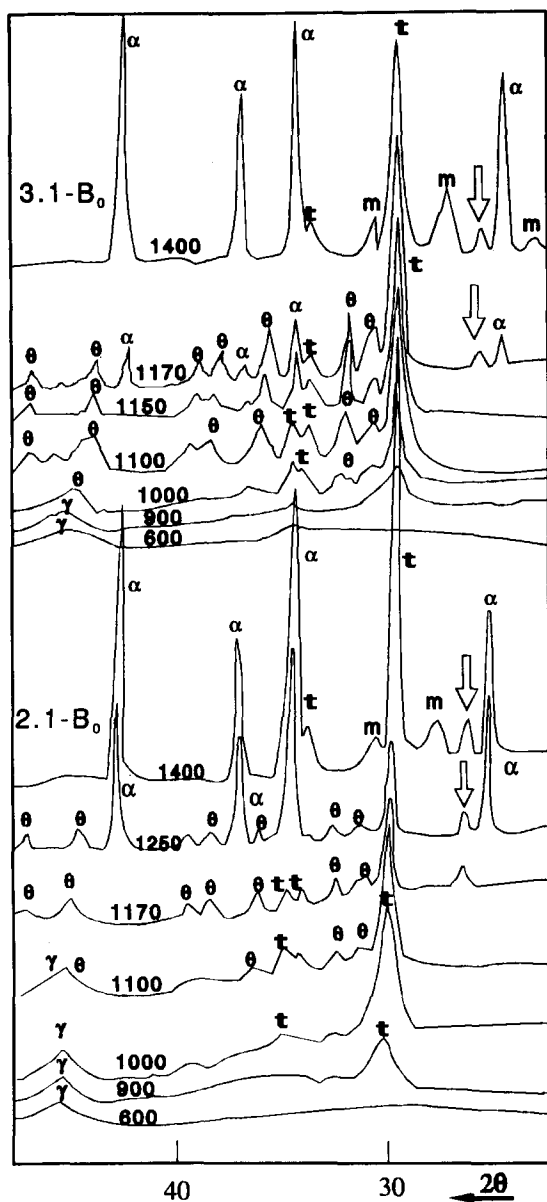


Fig. 3. X-Ray diffraction patterns of heat treated polymer matrix composites, 2.1-B<sub>0</sub> and 3.1-B<sub>0</sub>.

retains its tetragonal structure at temperatures up to 1250°C; even after heat treatment at 1400°C, less than 10 vol.% of the tetragonal phase had transformed to the monoclinic phase.

A new diffraction line ( $d = 3.35 \text{ \AA}$ ) appeared in the 2.1-B<sub>0</sub> sample heat treated at temperatures at and above 1170°C; this could not be attributed to any crystalline form of alumina and zirconia. The origin of this line will be discussed later.

The alumina and zirconia phase transformations in the 3.1-B<sub>0</sub> composite sample are similar to those in the 2.1-B<sub>0</sub> sample (Fig. 3), i.e. all the alumina and zirconia phase transformations are shifted to higher temperature than for the pure systems, but less strongly than in the case of the 2.1-B<sub>0</sub> composite (Fig. 3 and Table 3).

XRD patterns for the heated particulate matrix composite gels, 3.1-A<sub>0</sub> and 3.2-A<sub>0</sub>, are presented in Fig. 4. For both 3.1-A<sub>0</sub> and 3.2-A<sub>0</sub> samples the

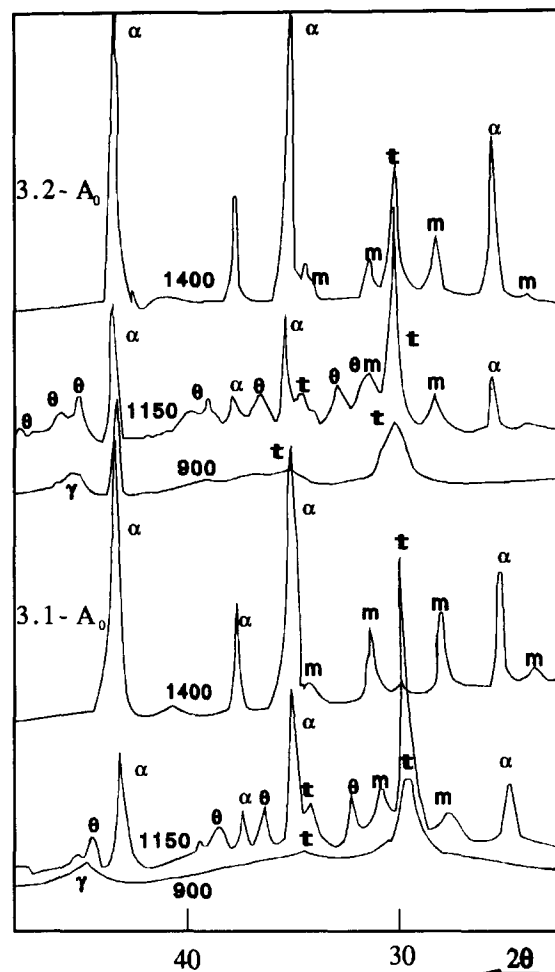


Fig. 4. X-Ray diffraction patterns of heat treated particulate matrix composites, 3.1-A<sub>0</sub> and 3.2-A<sub>0</sub>.

$\gamma$ -alumina is retained up to 900°C and the transformation  $\theta$ - to  $\alpha$ -alumina begins at 1150°C (lower temperatures than in the polymer matrix composites, 2.1-B<sub>0</sub> and 3.1-B<sub>0</sub>). As the transformation temperatures in pure particulate alumina<sup>24</sup> are higher (by about 50°C) than in the pure alkoxide-derived alumina<sup>20</sup> (Table 3), it is evident that the presence of zirconia in the particulate matrix composite does not have a pronounced influence on the alumina phase transformations. In both particulate composite samples, zirconia crystallized first in the tetragonal form (Fig. 4). The diffrac-

Table 4. Particle size broadening determined by the Scherrer equation ( $B_{(2\theta)} = 0.9 \lambda/L \cos \theta$ )<sup>a</sup>

	Size of ZrO <sub>2</sub> particles measured from tetragonal (111) line (nm)			
	2.1-B <sub>0</sub>	3.1-B <sub>0</sub>	3.1-A <sub>0</sub>	3.2-A <sub>0</sub>
900°C/1	6.7	7.5	9.4	8.9
1000°C/1	9.3	16.1	—	—
1100°C/1	15.8	18.2	—	—
1150°C/1	—	25.0	31.7	28.1
1170°C/1	25.7	34.2	—	—

<sup>a</sup>  $\lambda = 0.15418 \text{ nm}$ ,  $L =$  width at half-peak height in radians, and  $\theta =$  Bragg angle.

tion peaks of tetragonal zirconia at 900°C are sharper for the particulate matrix composites (Fig. 4) than for the polymer matrix composites (Fig. 3), probably indicating that tetragonal zirconia appears at a lower temperature. Zirconia particle sizes (Table 4) for the 3-1-A<sub>0</sub> and 3-2-A<sub>0</sub> samples are larger than for the 2-1-B<sub>0</sub> and 3-1-B<sub>0</sub> composites, and become significantly coarser with  $\alpha$ -alumina formation. Partial transformation of *t* → *m* zirconia consequently appears with formation of the  $\alpha$ -alumina at 1150°C. At higher temperatures, zirconia particles increase in size and the portion of monoclinic zirconia also increases.

In the XRD patterns of the particulate matrix composites, 3-1-A<sub>0</sub> and 3-2-A<sub>0</sub>, the diffraction line ( $d = 3.35 \text{ \AA}$ ) does not appear.

Generally according to the XRD results, an interaction between the phase transformations in the composites has been observed (i.e. there is influence of zirconia on the phase transformation of alumina and, in addition, the stability of the tetragonal zirconia in the alumina matrix is considerably changed, in respect to pure zirconia powder). Also, there is a remarkable difference in the alumina and zirconia phase transformations between the polymer matrix and the particulate matrix composites (Figs 3 and 4).

### 3.3 Microstructure of alumina-zirconia composite after heating

SEM micrographs of the 2-1-B<sub>0</sub> and 3-1-B<sub>0</sub> polymer matrix alumina-zirconia composites heat treated at 1400°C are presented in Fig. 5. Both composite samples are characterized by large alumina grains and by small intragranular zirconia particles. It is evident from Fig. 5(a) and (b) that the 2-1-B<sub>0</sub> composite exhibits much larger alumina grains than 3-1-B<sub>0</sub> composite. This may be a consequence of the higher  $\theta$ - to  $\alpha$ -alumina transformation temperature. On the other hand, the zirconia particles, in both polymer matrix samples heat treated at 1400°C, are mainly intragranularly distributed and have a very small size (average particle size is less than 0.2  $\mu\text{m}$ ). The zirconia particles are somewhat larger in the 2-1-B<sub>0</sub> than in the 3-1-B<sub>0</sub> composite (Fig. 5(c) and (d)), although, according to the XRD results (Fig. 3), a higher portion of monoclinic zirconia appears in the 3-1-B<sub>0</sub> sample heated at 1400°C. These differences could be attributed to the higher fraction of porosity in the 3-1-B<sub>0</sub> than in the 2-1-B<sub>0</sub> composite sample (Fig. 5).

The microstructures of the particulate matrix composites 3-1-A<sub>0</sub> and 3-2-A<sub>0</sub>, heat treated at 1400°C, are presented in Fig. 6. Microstructure with large alumina grains and intragranularly distributed zirconia particles is also visible. In Fig.

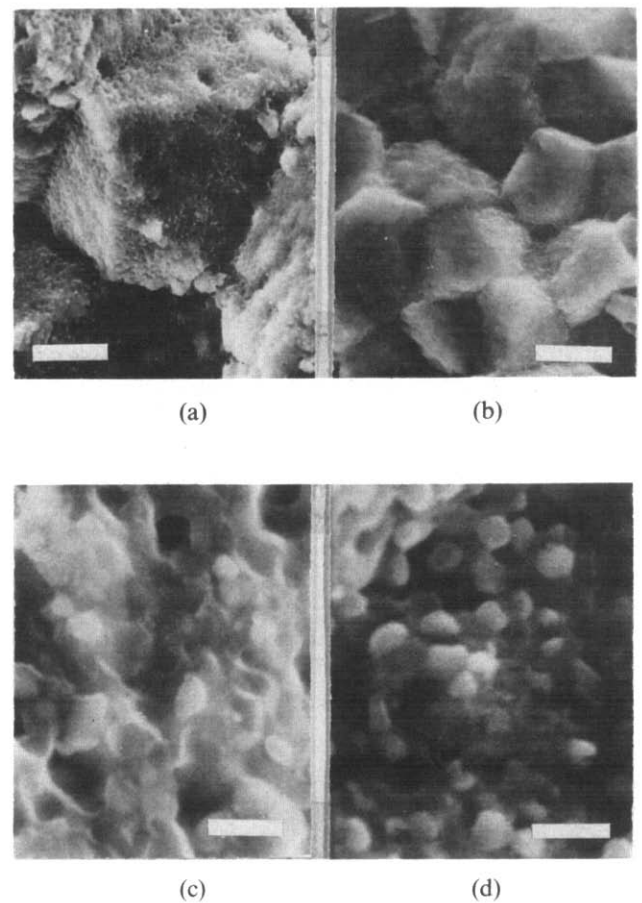


Fig. 5. SEM micrographs of the polymer matrix composites heat treated at 1400°C: (a) 2-1-B<sub>0</sub>, (b) 3-1-B<sub>0</sub> (bar = 5  $\mu\text{m}$ ), (c) 2-1-B<sub>0</sub> and (d) 3-1-B<sub>0</sub> (bar = 0.5  $\mu\text{m}$ ).

6(c) and (d) a small difference in the zirconia particle sizes is evident. As concerns the difference in the polymer (Fig. 5) and particulate (Fig. 6) matrix composite one can easily observe larger alumina grains and smaller zirconia particles in the polymer matrix composites than in the particulate ones.

These microstructural differences are results of the nature of the intimately bonded zirconia and alumina in the previous processing steps, which is discussed extensively in the next section.

### 3.4 Interactions between zirconia and alumina

These results indicate the existence of a mutual interaction between zirconia and alumina (especially the transitional forms of alumina), which is reflected in the phase transformations. This kind of interaction was mentioned by Pugar & Morgan<sup>8</sup> as an intimate association of Zr and Al via metal-oxygen-metal linkages. Low & McPherson reported<sup>9</sup> that in sol-gel derived alumina-zirconia composites, zirconia forms a solid solution with alumina and that the extent of the solid solution is greater than 5 wt% zirconia in  $\gamma$ -alumina, while it is less than 2 wt% in  $\alpha$ -alumina at 1300°C. In addition, it must be mentioned that because of the relatively large ionic radius of the zirconium with

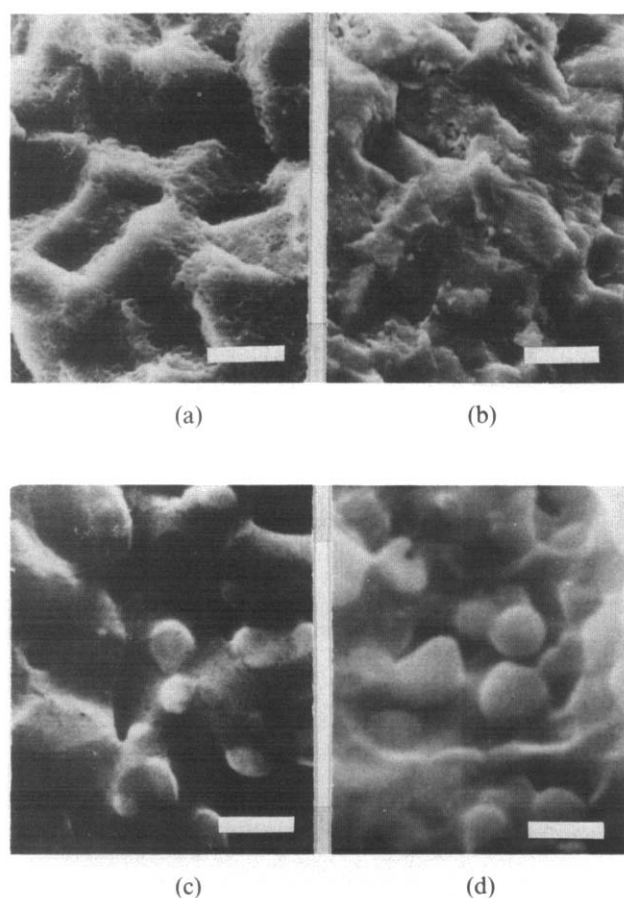


Fig. 6. SEM micrographs of the particulate matrix composites heat treated at 1400°C: (a) 3-1-A<sub>0</sub>, (b) 3-2-A<sub>0</sub> (bar = 5 μm), (c) 3-1-A<sub>0</sub> and (d) 3-2-A<sub>0</sub> (bar = 0.5 μm).

respect to that of the aluminium, and also because of classical composite processing with relatively large and dense particles, no appreciable solid solution of zirconia in alumina is expected.

The authors believe that if both alumina and zirconia original sol particles are small enough and with the more pronounced polymer alumina nature a gel network with intimate association of small boehmite and zirconia particles could be formed and many zirconium and aluminium atoms would be connected with metal–oxygen–metal linkages. It is expected that this very fine-scale mixed gel structure determines the structure of the heat treated samples, especially at low temperatures, where the defect transitional forms of alumina exist. Hence the  $\gamma$ -alumina can retain zirconia incorporated in its own structure; the amount of incorporated zirconia is higher as the original particle sizes (of both alumina and zirconia) are smaller, and as the alumina has a more pronounced polymer nature.

It is known that  $\gamma$ -alumina, which consists of a close-packed oxygen with both tetrahedral and octahedral interstices occupied by aluminium cations,<sup>25,26</sup> is more disordered if the portion of tetrahedral coordinated aluminium ions is higher. Thus, the evident 'poor crystallinity' of the  $\gamma$ -alu-

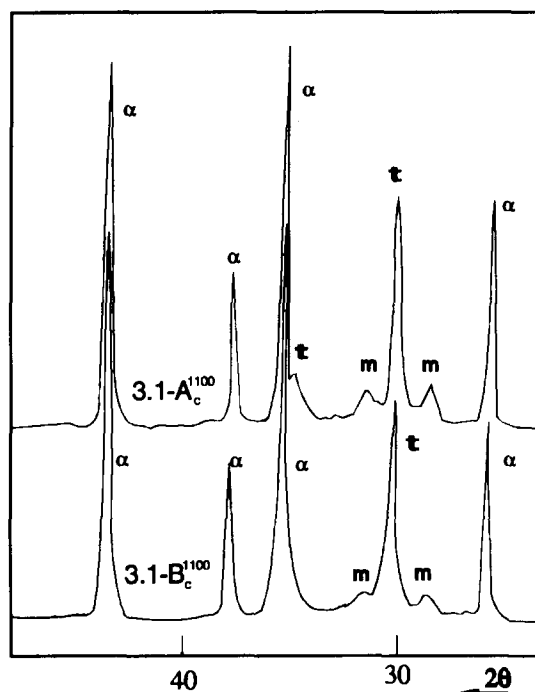


Fig. 7. X-Ray diffraction patterns of seeded alumina-zirconia composites heat treated at 1100°C (according to Ref. 16).

mina in the polymer matrix composites, 2-1-B<sub>0</sub> and 3-1-B<sub>0</sub> (Fig. 3), indicates a more disordered  $\gamma$ -alumina structure relative to the pure alkoxide derived alumina,<sup>20</sup> with high portion of tetrahedrally coordinated aluminium ions, perhaps as a consequence of the zirconium ions in the  $\gamma$ -alumina structure. In addition, as can be seen (Fig. 3) in the polymer matrix alumina–zirconia composites, the presence of zirconia stabilizes the  $\gamma$ -alumina even above 1000°C, a much higher temperature than for the pure alumina.<sup>20</sup>

In the polymer matrix composites, 2-1-B<sub>0</sub> and 3-1-B<sub>0</sub> (Fig. 3), tetragonal zirconia first appears at higher temperatures than in the pure zirconia powder.<sup>21–23</sup> That result indicates an intimate interaction of zirconia with alumina. Thus, zirconia is not able to form its own crystalline structure, insofar as it is in close association with  $\gamma$ -alumina structure.

The results in Section 3.2 suggest that the stability of tetragonal zirconia is decreased in the presence of  $\alpha$ -alumina. In order to explain this finding, it is necessary to compare the XRD results of these composite with the XRD results previously reported,<sup>17</sup> for the same composite samples, but seeded with  $\alpha$ -alumina particles. The seeding significantly decreases the temperature of the  $\theta$ - to  $\alpha$ -alumina phase transformation,<sup>12,17</sup> but at the same time, the partial t  $\rightarrow$  m zirconia phase transformation occurs, with the appearance of the  $\alpha$ -alumina at lower temperature too (Fig. 7).<sup>17</sup> Thus, in the seeded 3-1-B<sub>c</sub> and 3-1-A<sub>c</sub> composites, monoclinic zirconia appears already at temperatures

somewhat lower than 1100°C. This indicates that formation of the  $\alpha$ -alumina alters the stability of tetragonal zirconia.

In addition, as has already been mentioned, the presence of  $\gamma$ -alumina at relatively high temperature shifts the transformation temperatures to  $\theta$ - and to  $\alpha$ -alumina. This shifting is very pronounced in the polymer matrix composites (because of the very fine original boehmite particles with expressed polymer nature), and especially for the 2-1-B<sub>0</sub> sample, where the stronger mutual interaction between alumina and zirconia exists, because zirconium ions instead of zirconia particles were introduced in the polymer alumina matrix. As the particulate matrix composites, 3-1-A<sub>0</sub> and 3-2-A<sub>0</sub>, have originally larger and denser boehmite particles than the polymer matrix composites, 2-1-B<sub>0</sub> and 3-1-B<sub>0</sub>, it can be expected that interaction between the zirconia and  $\gamma$ -alumina will be smaller. This can explain why the shifting of the transformation temperature to  $\alpha$ -alumina is not as pronounced (Fig. 4 and Table 3), relative to the pure particulate alumina.<sup>24</sup>

The interaction between zirconia and alumina can be associated with the new diffraction line ( $d = 3.35 \text{ \AA}$ ) found in the polymer matrix composites. According to the XRD results (Fig. 3) the new line appears only in the polymer matrix composites at temperature above 1150°C. The intensity of the peak depends on the origin of zirconia particles and it is higher for the 2-1-B<sub>0</sub> than for the 3-1-B<sub>0</sub> polymer matrix composite; i.e. where the mutual interaction between zirconia and alumina is more pronounced. It is interesting to note that in the seeded polymer matrix composite,<sup>17</sup> the new diffraction line does not occur, which indicates that the presence of transitional form of alumina at relatively high temperature is necessary for its occurrence.

#### 4 Conclusions

It has been shown that in the sol-gel processing of the alumina-zirconia composites, there is an intimate interaction between the alumina and the zirconia. The zirconia particles change the route of the alumina phase transformations, shifting the stability of the  $\gamma$ -alumina, and consequently the stable  $\alpha$ -alumina formation, toward higher temperatures than in the pure alumina system (for up to 150°C). The degree of the zirconia influence depends on the origin of the zirconia particles and the nature of the alumina matrix.

In contrast, the nature of the alumina matrix has an influence on the mechanism and size of the zirconia particle formation and its phase stability.

Tetragonal zirconia does not appear until 900°C, and it is stable almost up to 1400°C.

#### References

1. Claussen, N., Fracture toughness of Al<sub>2</sub>O<sub>3</sub> with an unstabilized ZrO<sub>2</sub> dispersed phase. *J. Am. Ceram. Soc.*, **59** (1976) 49-51.
2. Bleier, A., Becher, P. F., Alexander, K. B. & Westmoreland, G. C., Effect of aqueous processing conditions of the microstructure and transformation behaviour in Al<sub>2</sub>O<sub>3</sub>-ZrO<sub>2</sub> (CeO<sub>2</sub>) composites. *J. Am. Ceram. Soc.*, **75** (1992) 2649-58.
3. Lange, F. F., Transformation toughening. *J. Mat. Sci.*, **17** (1982) 225-54.
4. Wang, J. & Stevens, R., Review—zirconia-toughened alumina (ZTA) ceramics. *J. Mat. Sci.*, **24** (1989) 3421-40.
5. Claussen, N. & Rühle, M., Design of transformation-toughened ceramics. In *Advances in Ceramics*, Vol. 3, *Science and Technology of Zirconia*, ed. A. H. Heuer & W. L. Hobbs. The American Ceramic Society, Columbus, OH, 1981, pp. 137-83.
6. Heuer, A. H., Claussen, N., Kriven, W. M. & Rühle, M., Stability of tetragonal ZrO<sub>2</sub> particles in ceramic matrices. *J. Am. Ceram. Soc.*, **65** (1982) 642-50.
7. Bond, W. D. & Becher, P. F., Synthesis of alumina-zirconia powders by sol-gel processing. In *Ultrastructure Processing of Ceramics, Glasses and Composites*, ed. MacKenzie & D. R. Ulrich, A. Wiley-Interscience Publ., NY, 1987, pp. 443-51.
8. Pugar, E. A. & Morgan, P. E. D., Coupled grain growth effect in Al<sub>2</sub>O<sub>3</sub>/10 vol.% ZrO<sub>2</sub>. *J. Am. Ceram. Soc.*, **69** (1986) C-120-3.
9. Low, I. M. & McPherson, R., Crystallization of gel derived alumina and alumina-Zirconia ceramics. *J. Mat. Sci.*, **24** (1989) 892-8.
10. Debsikdar, J. C., Influence of synthesis chemistry on alumina-zirconia powder characteristic. *J. Mat. Sci.*, **22** (1987) 2237-47.
11. Bach, J. P. & Thevenot, F., Fabrication and characterization on zirconia-toughened alumina obtained by inorganic and organic precursors. *J. Mat. Sci.*, **24** (1989) 2711-21.
12. Messing, G. L. & Kumagai, M., Low temperature sintering of seeded sol-gel derived ZrO<sub>2</sub>-toughened Al<sub>2</sub>O<sub>3</sub> composites. *J. Am. Ceram. Soc.*, **72** (1989) 40-44.
13. Srdić, V. & Radonjić, L., The microstructure control in the sol-gel derived alumina-zirconia composite. In *Proc. 4th Inter. Symp. Ceram. Mater. and Compon. for Engines*, ed. R. Carlsson. Elsevier Applied Science, London, 1991, pp. 277-83.
14. Yoldas, B. E., Alumina sol preparation from alkoxides. *Am. Ceram. Soc. Bull.*, **54** (1975) 289-90.
15. Yoldas, B. E., Alumina gels that form porous transparent Al<sub>2</sub>O<sub>3</sub>. *J. Mat. Sci.*, **10** (1975) 1856-60.
16. Srdić, V., Radonjić, L. & Bokorov, M., Microstructure development in sol-gel derived alumina-zirconia composites. In *8th SIMCER*, Rimini, Italy, November 1992.
17. Srdić, V. & Radonjić, L., Seeded sol-gel derived alumina-zirconia composites. *Ceram. Int.*, **20** (1994).
18. Toraya, H., Yoshimura, M. & Somiya, S., Calibration curve for quantitative analysis of the monoclinic-tetragonal ZrO<sub>2</sub> system by X-ray diffraction. *J. Am. Ceram. Soc.*, **67** (1984) C-119-21.
19. Warren, B. E., *X-Ray Diffraction*. Reading, Massachusetts, 1989, pp. 251-4.
20. Radonjić, L., Srdić, V. & Nikolić, L., Relationship between the microstructure of Boehmite gels and their transformation to alpha-alumina. *Mat. Chem. Phys.*, **33** (1993) 298-306.
21. Distler, W., Tomandl, G., Kohl, R., Stiegelschmitt, A. & Rinn, G., Processing of ZrO<sub>2</sub> ceramics from spherical

- powders obtained by sol-gel process. In *Euro-Ceramics*, ed. G. With, R. A. Terpstra & R. Metselaar. Elsevier Applied Science, London, 1989, pp. 1160-4.
22. Murase, Y., Kato, E. & Daimon, K., Stability of  $ZrO_2$  phases in ultrafine  $ZrO_2-Al_2O_3$  mixtures. *J. Am. Ceram. Soc.*, **69** (1986) 83-7.
  23. Kundu, P., Pal, D. & Sen, S., Preparation and thermal evolution of sol-gel derived transparent  $ZrO_2$  and  $MgO-ZrO_2$  gel monolith. *J. Mat. Sci.*, **23** (1988) 1539-46.
  24. Radonjić, L., Srdić, V. & Nikolić, L., Seeded transformation of alumina gels. In *Euro-Ceramics*, ed. G. Ziegler. Deutsche Keramische Gesellschaft, Augsburg, 1992, in print.
  25. Saraswati V., Rao, G. V. N. & Rao, G. V. R., Structural evolution in alumina gel. *J. Mat. Sci.*, **22** (1987) 2529-34.
  26. Nazar, L. & Klein, L., Early stage of alumina sol-gel formation. *J. Am. Ceram. Soc.*, **71** (1988) C-85.